Proceedings of ALGORITMY 2005
pp. 132–141

BASIC NUMERICAL TESTING OF MIXED HYBRID FE MODEL OF COMPRESSIBLE FLOW WITH ARTIFICIAL VISCOSITY*

JAN ŠEMBERA AND JIŘÍ MARYŠKA†

Abstract. The contribution is a follow-up to the paper of the same authors in Algoritmy 2002 Proceedings. It was concerned the numerical model of processes in a combustion engine. This contribution is devoted to one part of the model - a model of Eulerian compressible flow with artificial viscosity. The system of Euler, mass balance, and state equations is discretized in time using implicit finite difference method and in space using mixed hybrid formulation of finite element method. The artificial viscosity term is included and resulting system is linearized. Trilateral prismatic Raviart-Thomas finite elements are used. The definition of Raviart-Thomas approximation of weak solution of the Euler flow is set and results of a couple of numerical tests are presented.

Key words. mixed hybrid finite element method, computational fluid dynamics, artificial viscosity

AMS subject classifications. 76N15, 93A30, 65M60.

1. Introduction. In [6], overall review of a model of physical processes in a combustion engine and a short discussion of calibration of energy production were done. This contribution concentrates on one part of the model - a mixed hybrid finite element model of Eulerian compressible flow with artificial viscosity.

The problem of compressible isothermal flow of ideal gas is governed by the mass balance equation, Euler equation, and equation of state:

$$\frac{\partial}{\partial t}\varrho + \operatorname{div}(\varrho \mathbf{u}) = 0, \tag{1.1}$$

$$\frac{\partial}{\partial t}\mathbf{u} + (\mathbf{u}\cdot\mathbf{grad})\mathbf{u} = -\frac{1}{\varrho}\,\mathbf{grad}\; p + \mathbf{g}, \tag{1.2}$$

$$p = RT\varrho. \tag{1.3}$$

They should be held in domain Ω with Lipschitzian boundary Γ in time interval $\langle 0, \Delta t\rangle$ with boundary and initial conditions

$$p = p_{\mathrm{D}} \quad \text{on } \Gamma_{\mathrm{D}}, \tag{1.4}$$

$$\mathbf{u}\cdot\mathbf{n} = u_{\mathrm{N}} \quad \text{on } \Gamma_{\mathrm{N}}, \tag{1.5}$$

$$\mathbf{u}(\mathbf{x}) = \mathbf{u}_0(\mathbf{x}) \;\; ; \mathbf{x}\in\Omega, \tag{1.6}$$

$$p(\mathbf{x}) = p_0(\mathbf{x}) \;\; ; \mathbf{x}\in\Omega, \tag{1.7}$$

where $\Gamma = \Gamma_{\mathrm{D}} \cup \Gamma_{\mathrm{N}}$, $\Gamma_{\mathrm{D}} \cap \Gamma_{\mathrm{N}} = \emptyset$, and $\mathbf{n}$ is outward unitary normal vector of the boundary Γ.

2. Isothermal Euler flow model with artificial viscosity. Let us derive the mixed hybrid weak solution of the problem. We use the technique applied to another physical problem in e.g. [1], [2], [4], [5]: decomposition of the domain Ω

*This work was supported with the subvention from Ministry of Education of the Czech Republic, project code MSM 242200001.

†Department of Modelling of Processes, Technical University of Liberec, Hálkova 16, 461 17 Liberec, Czech Republic (jan.sembera@vslib.cz).

into elements, definition of weak solution of system (1.1)–(1.7) on each element and appending conditions of transmission between neighbouring elements.

For this purpose denote E_h disjuct system of open sets (trilateral prisms - elements) covering the domain Ω: $\cup_{e\in E_h}\bar{e} = \bar{\Omega}\&(\forall e, e^* \in E_h)(e \neq e^* \Rightarrow e \cap e^* = \emptyset)$. Let Γ_h be the set of points on interelement sides except of the ones, where Dirichlet boundary condition is prescribed $\Gamma_h = \bigcup_{e\in E_h} \partial e - \Gamma_D$ and $J_h = \{f; (\exists (e, e^*) \in E_h \times E_h)(f = \bar{e} \cap \bar{e^*}) \vee (\exists e \in E_h)(f = \bar{e} \cap \Gamma)\}$ is set of all element sides.

Further let $\mathbf{RT}_{E_h}$ be the Raviart-Thomas space and let $\mathbf{M}_{E_h}$ and $\mathbf{M}_{\Gamma_h}$ be the multiplicator spaces:

$$\begin{aligned}\mathbf{RT}_{E_h} &= \mathrm{span}\{\mathbf{w}_j^e; j \in \{0,1,2,3,4\}, e \in E_h\},\\ \mathbf{M}_{E_h} &= \mathrm{span}\{\Phi^e; e \in E_h\},\\ \mathbf{M}_{\Gamma_h} &= \mathrm{span}\{\varphi_f; f \in J_h\},\end{aligned}$$

where

$$\mathbf{w}_j^e(x,y,z) = \begin{cases} k_j^e \begin{pmatrix} x - a_j^e \\ y - b_j^e \\ z - c_j^e \end{pmatrix} & \text{for } (x,y,z) \in e \\ 0 & \text{else} \end{cases}, j = 0,\dots,4, \tag{2.1}$$

$$\Phi^e(x,y,z) = \begin{cases} 1 & \text{for } (x,y,z) \in e \\ 0 & \text{else} \end{cases}, \tag{2.2}$$

$$\varphi_f(x,y,z) = \begin{cases} 1 & \text{for } (x,y,z) \in f \\ 0 & \text{else} \end{cases}, \tag{2.3}$$

and coefficients k_j^e, a_j^e, b_j^e, c_j^e are defined by requirement of fulfilling the equalities

$$\int_{\partial_j^e} \gamma_{\partial e}\mathbf{w}_i^e \cdot \mathbf{n}^e = \delta_{ij}, \quad i,j = 0,\dots,4, \tag{2.4}$$

where $\gamma_{\partial e}$ is the operator of trace and ∂_j^e means j^{th} side of element e. We remind that each trilateral prismatic element $e \in E_h$ has 5 sides (they are numbered by index j).

After that we complete the model with a term of "artificial viscosity" estimating energy transfer due to viscosity. Its form is derived from the form of viscous term in Raviart-Thomas approximation of Navier-Stokes flow. Its value is modified by artificial viscosity weight K_η. The following definition contains the resulting form of problem:

DEFINITION 2.1. *We say that the system of functions* $(\mathbf{f}_h, \mathbf{u}_h, p_h, \varrho_h, \lambda_h) \in \mathbf{RT}_{E_h} \times \mathbf{RT}_{E_h} \times \mathbf{M}_{E_h} \times \mathbf{M}_{E_h} \times \mathbf{M}_{\Gamma_h}$ *is the Raviart-Thomas approximation of weak solution of mixed hybrid formulation of the Euler isothermal flow problem with artificial viscosity with artificial viscosity weight* K_η*, if for all test functions* $(\mathbf{w}_h, \mathbf{v}_h, \phi_h, \varphi_h, \mu_h) \in \mathbf{RT}_{E_h} \times \mathbf{RT}_{E_h} \times \mathbf{M}_{E_h} \times \mathbf{M}_{E_h} \times \mathbf{M}_{\Gamma_h}$ *hold*

$$\begin{aligned}&\sum_{e\in E_h}\left[\int_e\left(\frac{1}{\Delta t}\mathbf{f}_h + (\mathbf{f}_h \cdot \mathbf{grad})\ \mathbf{u}_h\right)\cdot \mathbf{w}_h + K_\eta \sum_{i=1}^{3}\int_e \eta \mathbf{grad}\ u_{h,i} \cdot \mathbf{grad}\ w_{h,i} - \right.\\ &\left. -\int_e p_h \mathrm{div}\ \mathbf{w}_h + \int_{\partial e\cap\Gamma_h} \lambda_h \gamma_{\partial e}(\mathbf{w}_h|_e)\cdot \mathbf{n}^e\right] = \sum_{e\in E_h}\left(\frac{1}{\Delta t}\int_e \varrho_h \mathbf{u}_{(i),h}\cdot \mathbf{w}_h - \right.\\ &\left. - \int_{\partial e\cap\Gamma_D} p_{D,h}\gamma_{\partial e}(\mathbf{w}_h|_e)\cdot \mathbf{n}^e + \int_e \varrho_h \mathbf{g}\cdot \mathbf{w}_h\right),\end{aligned} \tag{2.5}$$

$$\sum_{e\in E_h}\left[-\int_e \operatorname{div}\,\mathbf{f}_h\phi_h-\frac{1}{\Delta t}\int_e \varrho_h\phi_h\right]=-\frac{1}{\Delta t}\sum_{e\in E_h}\int_e \varrho_{(i),h}\phi_h, \tag{2.6}$$

$$0=\sum_{e\in E_h}\int_e (RT\varrho_h-p_h)\varphi_h, \tag{2.7}$$

$$0=\sum_{e\in E_h}\int_e (\varrho_h\mathbf{u}_h-\mathbf{f}_h)\cdot\mathbf{v}_h, \tag{2.8}$$

$$\sum_{e\in E_h}\left(\int_{\partial e\cap\Gamma_{\mathrm{N}}}\mu_h\gamma_{\partial e}(\mathbf{u}_h|_e)\cdot\mathbf{n}^e-\int_{\partial e\cap\Gamma_{\mathrm{N}}}\sigma\lambda_h\mu_h\right)=\sum_{e\in E_h}\int_{\partial e\cap\Gamma_{\mathrm{N}}}(u_{\mathrm{N},h}-\sigma p_{\mathrm{D},h})\mu_h. \tag{2.9}$$

Let us remark that new variable function λ_h was introduced to the model as approximation of pressure trace on Γ_h.

The system (2.5)–(2.9) can be rewritten in the following block matrix form:

$$\begin{pmatrix} \mathrm{A}(\vec{p},\vec{f})+K_\eta\mathrm{V}(\vec{p}) & \mathrm{B} & \mathrm{C}\\ \mathrm{B}^{\mathrm{T}} & \mathrm{D} & \mathbf{0}\\ \mathrm{C}^{\mathrm{T}} & \mathbf{0} & \mathrm{E}\end{pmatrix}\begin{pmatrix}\vec{f}\\ \vec{p}\\ \vec{\lambda}\end{pmatrix}=\begin{pmatrix}\vec{r}_1(\vec{p})\\ \vec{r}_2\\ \vec{r}_3\end{pmatrix},$$

where $\vec{f}$ (dimension $5|E_h|$), $\vec{p}$ (dimension $|E_h|$), and $\vec{\lambda}$ (dimension $|J_h|$) are vectors of interlement fluxes, pressure in elements, and pressure on element sides respectively, $\vec{r}_1$, $\vec{r}_2$, and $\vec{r}_3$ are vectors of right hand sides, and nonlinear term $\mathrm{A}(\vec{p},\vec{f})+K_\eta\mathrm{V}(\vec{p})$ of dimensions $5|E_h|\times 5|E_h|$ is block diagonal with 5×5 blocks (matrix $\mathrm{V}(\vec{p})$ itself is symmetric), matrix B of dimensions $5|E_h|\times|E_h|$ is block diagonal with 5×1 blocks, C of dimensions $5|E_h|\times|J_h|$ contains at most two nonzeros in each column, and matrices D (type $|E_h|\times|E_h|$) and E (type $|J_h|\times|J_h|$) are diagonal.

3. Linearization. The equation (2.5) contains nonlinear terms. Two variants of linearization derived from linearized implicit method approach [3] were tested. We call them according to the main difference between resulting linear equation systems as "symmetric" and "nonsymmetric" linearization.

Symmetric linearization corresponds to substitution of term $(\mathbf{u}\cdot\mathbf{grad})\,\mathbf{u}$ in Euler equation by the product $(\mathbf{u}\cdot\mathbf{grad})\,\breve{\mathbf{u}}$, where $\breve{\mathbf{u}}$ represents a priori estimate of velocity $\mathbf{u}$, and substitution of pressure in resting nonlinear terms by its a priori estimate (actual value of it in our computations is specified in algorithm 1). Resulting system can be rewritten in the block matrix form as follows:

$$\begin{pmatrix} \mathbf{A}^S(\breve{\vec{p}},\breve{\vec{f}})+K_\eta\mathrm{V}(\breve{\vec{p}}) & \mathbf{B} & \mathbf{C}\\ \mathbf{B}^{\mathrm{T}} & \mathbf{D} & \mathbf{0}\\ \mathbf{C}^{\mathrm{T}} & \mathbf{0} & \mathbf{E}\end{pmatrix}\begin{pmatrix}\vec{f}\\ \vec{p}\\ \vec{\lambda}\end{pmatrix}=\begin{pmatrix}\vec{r}_1(\breve{\vec{p}})\\ \vec{r}_2\\ \vec{r}_3\end{pmatrix}. \tag{3.1}$$

Here matrix $\mathbf{A}^S$ is always symmetric and consequently the whole system matrix is symmetric.

Nonsymmetric linearization substitutes the term $(\mathbf{u}\cdot\mathbf{grad})\,\mathbf{u}$ in Euler equation by the term $(\breve{\mathbf{u}}\cdot\mathbf{grad})\,\mathbf{u}$. The linear algebraic system is then written as

$$\begin{pmatrix} \mathbf{A}^N(\breve{\vec{p}},\breve{\vec{f}})+K_\eta\mathrm{V}(\breve{\vec{p}}) & \mathbf{B} & \mathbf{C}\\ \mathbf{B}^{\mathrm{T}} & \mathbf{D} & \mathbf{0}\\ \mathbf{C}^{\mathrm{T}} & \mathbf{0} & \mathbf{E}\end{pmatrix}\begin{pmatrix}\vec{f}\\ \vec{p}\\ \vec{\lambda}\end{pmatrix}=\begin{pmatrix}\vec{r}_1(\breve{\vec{p}})\\ \vec{r}_2\\ \vec{r}_3\end{pmatrix}. \tag{3.2}$$

Here the symmetry of matrix $\mathbf{A}^N$ and thus the whole system matrix is not guaranteed.

The system (3.1) or (3.2) is solved using the following iterative process:

ALGORITHM 1. *For $k = 0, \dots, K-1$, we solve the system*

$$\begin{pmatrix} \mathbf{A}(\breve{\vec{p}}^{[k]}, \breve{\vec{f}}^{[k]}) + K_\eta \mathrm{V}(\breve{\vec{p}}^{[k]}) & \mathbf{B} & \mathbf{C} \\ \mathbf{B}^{\mathrm{T}} & \mathbf{D} & \mathbf{0} \\ \mathbf{C}^{\mathrm{T}} & \mathbf{0} & \mathbf{E} \end{pmatrix} \begin{pmatrix} \vec{f}^{[k+1]} \\ \vec{p}^{[k+1]} \\ \vec{\lambda}^{[k+1]} \end{pmatrix} = \begin{pmatrix} \vec{r}_1(\breve{\vec{p}}^{[k]}) \\ \vec{r}_2 \\ \vec{r}_3 \end{pmatrix},$$

where $\mathbf{A}$ is either $\mathbf{A}^S$ or $\mathbf{A}^N$ and $\breve{\vec{p}}^{[0]} = \vec{p}^{[0]}$ and $\breve{\vec{f}}^{[0]} = \vec{f}^{[0]}$ represent the initial conditions. The components of vectors $\breve{\vec{p}}^{[k+1]} = (\breve{p}^{e_0}_{[k+1]}, \breve{p}^{e_1}_{[k+1]}, \dots, \breve{p}^{e_{|E_h|}}_{[k+1]})^T$, $\breve{\vec{f}}^{[k+1]} = (\breve{f}^{e_0}_{[k+1],0}, \dots, \breve{f}^{e_0}_{[k+1],4}, \dots, \breve{f}^{e_{|E_h|}}_{[k+1],0}, \dots, \breve{f}^{e_{|E_h|}}_{[k+1],4})^T$ are defined by

$$\breve{p}^e_{[k+1]} = \breve{p}^e_{[k]} + \omega(\bar{p}^e_{[k+1]} - \breve{p}^e_{[k]}), \text{ where } \bar{p}^e_{[k+1]} = \tilde{p}^e_{[0]} + \alpha(\tilde{p}^e_{[k+1]} - \tilde{p}^e_{[0]})$$
$$\breve{f}^e_{[k+1],j} = \breve{f}^e_{[k],j} + \omega(\bar{f}^e_{[k+1],j} - \breve{f}^e_{[k],j}), \text{ where } \bar{f}^e_{[k+1],j} = \tilde{f}^e_{[0],j} + \alpha(\tilde{f}^e_{[k+1],j} - \tilde{f}^e_{[0],j}).$$

The number of iteration steps K is given by stopping condition

$$(\forall e \in E_h)(\forall j \in \{0, \dots, 4\})(|\breve{p}^e_{[K]} - \breve{p}^e_{[K-1]}| \le \varepsilon \ \ \& \ \ |\breve{f}^e_{[K],j} - \breve{f}^e_{[K-1],j}| \le \varepsilon). \tag{3.3}$$

DEFINITION 3.1. *Applying the algorithm 1, we call the triple of vectors $(\vec{f}, \vec{p}, \vec{\lambda}) = (\vec{f}^{[K]}, \vec{p}^{[K]}, \vec{\lambda}^{[K]})$, the approximation of solution of Raviart-Thomas approximation of weak solution of mixed hybrid formulation of the Euler isothermal flow problem.*

Further details can be found in [7].

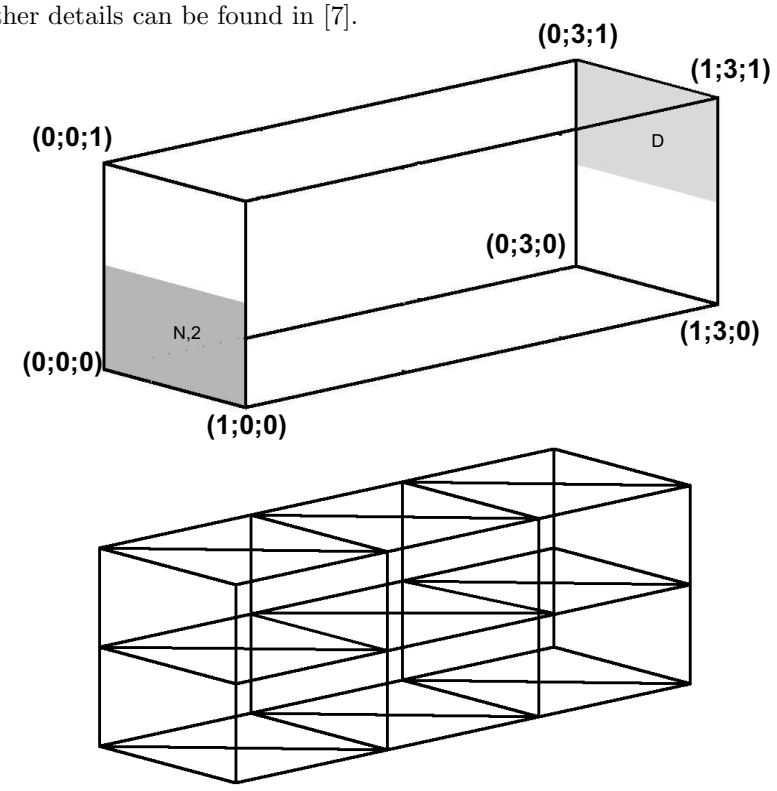

FIG. 3.1. *Region Ω with marked boundary parts $\Gamma_{\mathrm{N},2}$ and Γ_{D} and shape of the used discretization mesh.*

4. First results of artificial viscosity testing. Since the computations are very expensive in CPU time, we started with the small mesh composed of 12 finite elements. The domain Ω and partioning of its boundary is following (see Fig. 3.1):

$$\begin{aligned}
\Omega &= \langle 0;1\rangle \times \langle 0;3\rangle \times \langle 0;1\rangle,\\
\Gamma_{\mathrm{N},1} &= \{0;1\} \times \langle 0;3\rangle \times \langle 0;1\rangle \cup \langle 0;1\rangle \times \langle 0;3\rangle \times \{0;1\} \cup\\
&\quad \cup \langle 0;1\rangle \times \{0\} \times \langle 0;0.5\rangle \cup \langle 0;1\rangle \times \{3\} \times (0.5;1\rangle,\\
\Gamma_{\mathrm{N},2} &= \langle 0;1\rangle \times \{0\} \times \langle 0.5;1\rangle,\\
\Gamma_{\mathrm{D}} &= \langle 0;1\rangle \times \{3\} \times \langle 0;0.5\rangle.
\end{aligned}$$

The form of the boundary and initial conditions is:

$$\begin{aligned}
p &= 99990 \quad \text{on } \Gamma_{\mathrm{D}},\\
\mathbf{u}\cdot\mathbf{n} &= 0 \quad \text{on } \Gamma_{\mathrm{N},1},\\
\mathbf{u}\cdot\mathbf{n} &= -0.2 \quad \text{on } \Gamma_{\mathrm{N},2},\\
\mathbf{u}(0,\mathbf{x}) &= 0 \quad ; \mathbf{x} \in \Omega,\\
p(0,\mathbf{x}) &= 100000 \quad ; \mathbf{x} \in \Omega.
\end{aligned}$$

The values of T and R are constant, $T = 300$, $R = 668.8$.

Testing was made using two lengths of time step Δt. The "long time step" $\Delta t = 500$ was applied computing problem in the time interval $\langle 0, 2000\rangle$ and the "short time step" $\Delta t = 0.005$ when computing problem on the time interval $\langle 0;2\rangle$.

The computations were made with symmetric (3.1) and nonsymmetric (3.2) linearization. Parameters of iterative process were $\alpha = 1$, $\omega = 0.4$, $\varepsilon = 10^{-9}$.

The computations with artificial viscosity were made with parameters $\eta = 10^{-3}$ and $K_\eta = 10^5$, the computations without artificial viscosity correspond to artificial viscosity weight $K_\eta = 0$.

The linear algebraic systems were solved using Gauss elimination method.

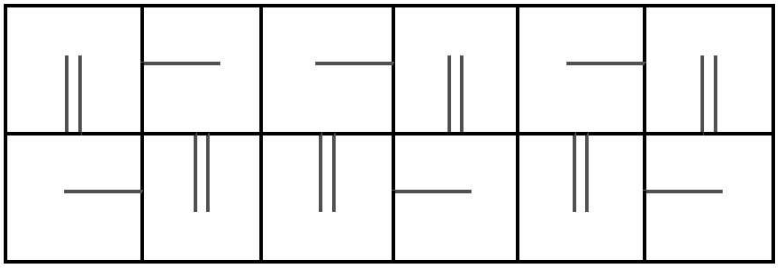

FIG. 4.1. *Visualization of fluxes between mesh elements in vertical cut of the domain Ω in time $t = 2000$ computed using time step $\Delta t = 500$ and symmetric linearization without artificial viscosity (the scale is about 1000 times larger than in figures 4.2 and 4.3. That is why the boundary fluxes on $\Gamma_{\mathrm{N},2}$ and Γ_{D} are not visible). Unitary normal component of velocity is represented by length about 0.035* mm.

All tests made with long time step $\Delta t = 500$ demonstrated common attributes of flow field in time $t = 2000$ (following statements hold relatively to the computer accuracy): the fluxes through the impermeable part of boundary $\Gamma_{\mathrm{N},1}$ are zero, fluxes through permeable boundary parts $\Gamma_{\mathrm{N},2}$ and Γ_{D} have the same size corresponding to the prescribed boundary condition on $\Gamma_{\mathrm{N},2}$ and the same direction coincident with y

TABLE 4.1
Comparison of various results of "small mesh" problem.

computation	flow field	min. /max. pressure	number of iterations
symmetric without viscosity	Fig. 4.1	99990 / 141613	133/92/71/54
nonsymmetric without viscosity	Fig. 4.2	99990 / 99990	49/10/6/2
symmetric with viscosity	Fig. 4.3	99996 / 100023	38/8/1/1
nonsymmetric with viscosity	Fig. 4.3	99996 / 100023	38/8/1/1

axis. The flow field is conservative (the sum of fluxes through all sides of each element is zero).

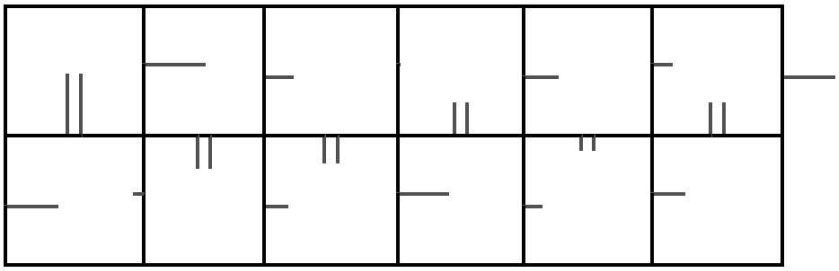

FIG. 4.2. *Visualization of fluxes between mesh elements in vertical cut of the domain* Ω *in time* $t = 2000$ *computed using time step* $\Delta t = 500$ *and nonsymmetric linearization without artificial viscosity. Unitary normal component of velocity is represented by length about 35* mm.

The results differed in actual form of flow field, in extreme values of pressure and in number of iterations before the solution converged (see Tab. 4.1). The last column of the table contains the information on number of iterations computed in four time steps in the time interval $\langle 0; 2000 \rangle$.

Let us remark that in figures 4.1–4.6 the size of interelement fluxes is visualised quite non-standard way. The figures show a vertical cross-section of the mesh (rectangles) and lines orthogonal to faces of rectangles representing fluxes. They are oriented from the face to direction of flux and their length is proportional to flux amplitude. The number of flux lines (one or two) does not express any studied quality.

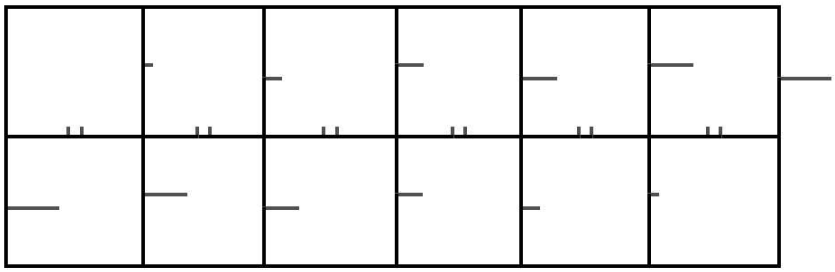

FIG. 4.3. *Visualization of fluxes between mesh elements in vertical cut of the domain* Ω *in time* $t = 2000$ *computed using time step* $\Delta t = 500$ *and symmetric or nonsymmetric linearization with artificial viscosity. Unitary normal component of velocity is represented by length about 35* mm.

The results demonstrate that when using long time step (looking for stationary solution), the artificial viscosity stabilisates the solution. The results of computations using symmetric and nonsymmetric linearization without artificial viscosity are dom-

inated (in the first case especially substantially) by vortices. Their form differs in the demonstrated computations, which implies idea that the vortices are generated by numerical noise comming from iteration process. Here can be registered the consequence of absence of the energy equation in the model and thus nonrespecting of energy conservation law. The results of both computations with artificial viscosity almost do not differ and there do not appear vortices in the flow field. The artificial viscosity manifests this property as should the real viscosity do.

FIG. 4.4. *Visualization of fluxes between mesh elements in vertical cut of the domain* Ω *in time* $t = 2$ *computed using time step* $\Delta t = 0.005$ *and nonsymmetric linearization without artificial viscosity. Unitary normal component of velocity is represented by length about 35* mm.

The results of tests using short time step $\Delta t = 0.005$ show fulfilling of boundary conditions, i.e. the fluxes through impermeable part of boundary $\Gamma_{\mathrm{N},1}$ are zero, the size of fluxes through permeable boundary $\Gamma_{\mathrm{N},2}$ corresponds to boundary conditions. The results of both computations without artificial viscosity oscillate in the whole interval $\langle 0; 2\rangle$ (in each time step the iteration process needs 3 iteration steps to determine new form of flow field) and differ mutually. The results of both computations with artificial viscosity steadied in time $t = 0.25$ and they are identical.

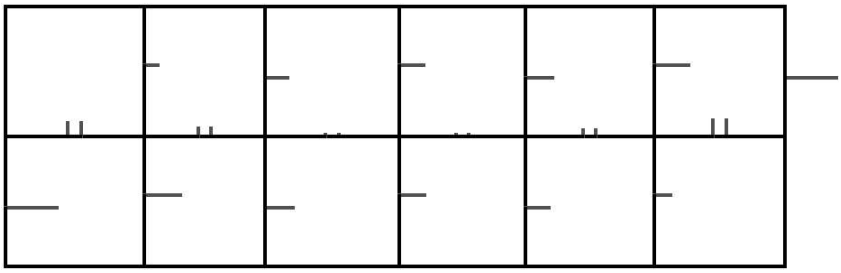

FIG. 4.5. *Visualization of fluxes between mesh elements in vertical cut of the domain* Ω *in time* $t = 2$ *computed using time step* $\Delta t = 0.005$ *and symmetric linearization without artificial viscosity. Unitary normal component of velocity is represented by length about 35* mm.

Figures 4.4–4.6 show the interelement fluxes in time $t = 2$ in various variants of the computation. The pressure field in both computations without artificial viscosity is even, in the whole volume pressure is equal to the Dirichlet boundary condition 99990. In both computations with artificial viscosity, the pressure field steadies with extrema 99996 and 100023.

Also here, the artificial viscosity has stabilising effect similarly to a natural image of the real viscosity.

FIG. 4.6. *Visualization of fluxes between mesh elements in vertical cut of the domain* Ω *in time* $t = 2$ *computed using time step* $\Delta t = 0.005$ *and symmetric and nonsymmetric linearization with artificial viscosity. Unitary normal component of velocity is represented by length about 35* mm.

Further testing was made on larger mesh with 226 elements discretizing the domain $\Omega = \langle 0; 2\rangle \times \langle 0; 2\rangle \times \langle 0; 0.1\rangle$, whose boundary is decomposed as follows (see Fig. 4.7):

$$\begin{aligned}\Gamma_{\mathrm{N},1} &= \langle 0; 2\rangle \times \{0; 2\} \times \langle 0; 0.1\rangle \cup \langle 0; 2\rangle \times \langle 0; 2\rangle \times \{0; 0.1\} \cup \\ &\quad \cup \{0\} \times \langle 0; 16/9) \times \langle 0; 0.1\rangle \cup \{2\} \times (2/9; 2\rangle \times \langle 0; 0.1\rangle, \\ \Gamma_{\mathrm{N},2} &= \{0\} \times \langle 16/9; 2\rangle \times \langle 0; 0.1\rangle, \\ \Gamma_{\mathrm{D}} &= \{2\} \times \langle 0; 2/9\rangle \times \langle 0; 0.1\rangle.\end{aligned}$$

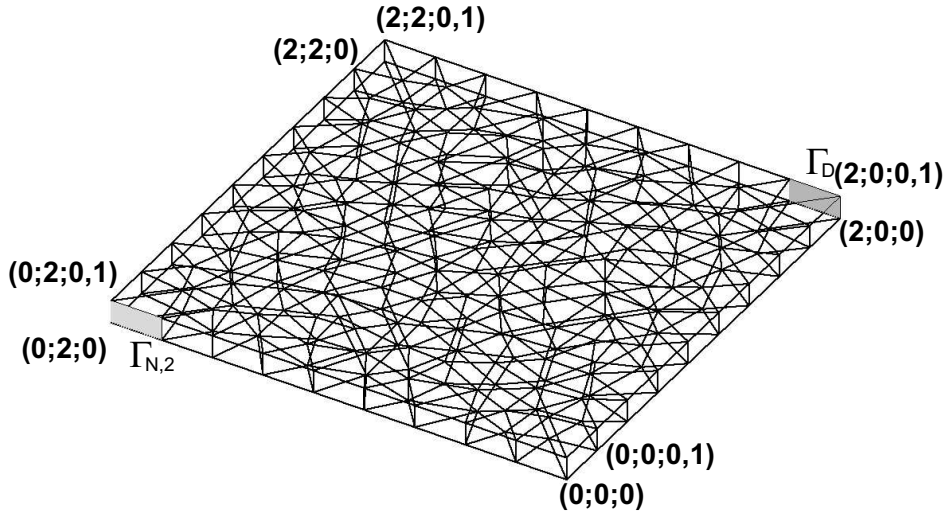

FIG. 4.7. *Region* Ω *with marked boundary parts* $\Gamma_{\mathrm{N},2}$ *and* Γ_{D} *and used discretization mesh.*

The boundary and initial conditions are

$$\begin{aligned} p &= 99990 \quad \text{on } \Gamma_{\mathrm{D}}, \\ \mathbf{u}\cdot\mathbf{n} &= 0 \qquad \text{on } \Gamma_{\mathrm{N},1}, \\ \mathbf{u}\cdot\mathbf{n} &= -4.5 \quad \text{on } \Gamma_{\mathrm{N},2}, \\ \mathbf{u}(0,\mathbf{x}) &= 0 \qquad ; \mathbf{x} \in \Omega, \\ p(0,\mathbf{x}) &= 100000 \quad ; \mathbf{x} \in \Omega. \end{aligned}$$

The values of T and R are constant: $T = 300$, $R = 668.8$.

The problem was solved in time interval $\langle 0; 0.4\rangle$ using time step $\Delta t = 0.01$ and symmetric linearization (3.1). Iteration parameters were chosen as $\alpha = 0.5$, $\omega = 1$, $\varepsilon = 5 \cdot 10^{-5}$.

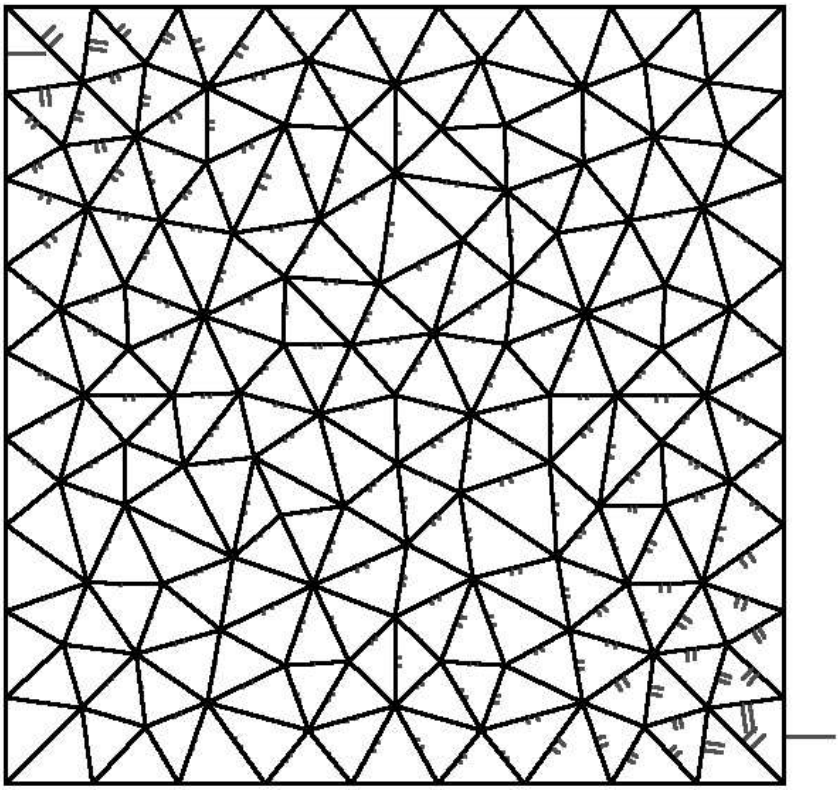

FIG. 4.8. *Visualization of interelement fluxes in horizontal cut of* Ω *in time* $t = 0.34$ *using* $K_\eta = 10^7$. *The lines orthogonal to faces of triangles represent fluxes. They are oriented from the face to direction of flux and their length is proportional to flux amplitude. The number of flux lines (one or two) does not express any studied quality.*

The linear algebraic equation systems were solved by external iterative solver based on preconditioned conjugate gradient method.

The size of viscosity was set to $\eta = 10^{-3}$. The influence of size of artificial viscosity weight K_η was observed. The computations were made with artificial viscosity weight $K_\eta = 0$, $K_\eta = 10^2$, $K_\eta = 10^5$, and $K_\eta = 10^7$ (the case $K_\eta = 0$ is equivalent to computation without artificial viscosity).

The results of computations with various sizes of artificial viscosity weight do not considerably differ in form of flow field. Figure 4.8 shows the flow field in time $t = 0.34$ for $K_\eta = 10^7$. There occure initial oscilations of velocity of gas outflow through Γ_{D} when $K_\eta = 0$. Their amplitude decrease as weight K_η increases. Similar oscilations can be observed in pressure field. Figure 4.9 shows plot of time evolution of pressure in the center of domain Ω. There is visible the same trend of pressure evolution with different amplitude of oscilations. Increasing artificial viscosity trend mutes the oscilations.

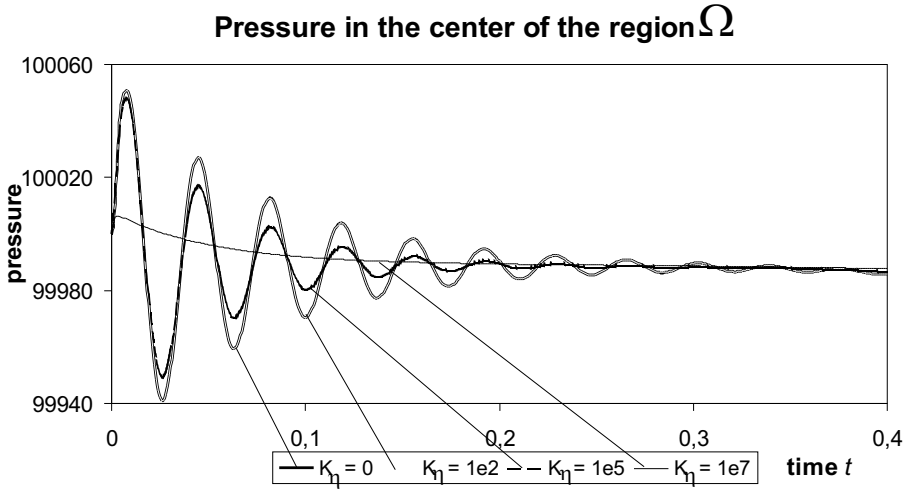

FIG. 4.9. *Comparison of time evolution of pressure in point (1;1;0.05) of computations with different artificial viscosity weights (the results for $K_\eta = 0$ and $K_\eta = 10^2$ coincide).*

5. Conclusion. The mixed hybrid finite element model of Eulerian compressible flow with artificial viscosity was defined and the influence of artificial viscosity was tested on two basic problems. The artificial viscosity demonstrates its stabilizing effect, especially reduction of spurious vortices in steady solutions and reduction of ocilations in unsteady problems. These results support the proposed form of artificial viscosity for mixed hybrid finite elements.

Further study of the proposed model should focus on possibility of calibration of the artificial viscosity weight for modelling viscous gas flow.

REFERENCES

[1] T. ARBOGAST AND Z. CHEN, *On the implementation of mixed methods as nonconforming methods for second-order elliptic problems*, Mathematics of Computation, 64 (1995), no. 211, pp. 943–972.

[2] T. ARBOGAST, M. F. WHEELER, AND N.-Y. ZHANG, *A nonlinear mixed finite element method for a degenerate parabolic equation arising in flow in porous media*, SIAM J. Numer. Anal., 33 (1996), no. 4, pp. 1669–1687.

[3] H. C. ELMAN, D. J. SILVESTER, AND A. J. WATHEN, *Iterative methods for problems in computational fluid dynamics*, Iterative Methods in Scientific Computing, Springer-Verlag, Singapore, 1997.

[4] J. MARYŠKA, M. ROZLOŽNÍK, AND M. TŮMA, *Mixed-hybrid finite-element approximation of the potential fluid-flow problem*, J. Comput. Appl. Math., 63 (1995), pp. 383–392.

[5] ———, *Schur complement systems in the mixed-hybrid finite element approximation of the potential fluid flow problem*, SIAM J. Sci. Comput., 22 (2000), pp. 704–723.

[6] J. ŠEMBERA AND J. MARYŠKA, *Discussion on numerical modelling of physical processes in a combustion engine*, in Proceedings of ALGORITMY 2002 (Bratislava, Slovakia), K. Mikula et al., eds., Slovak University of Technology, 2002, pp. 179–186.

[7] J. ŠEMBERA, *Aplikace MKP a MKO při studiu transportních jevů v proudícím plynu v proměnné oblasti* [in Czech], Ph.D. thesis, Department of Mathematics, FNSPE, Czech Technical University in Prague, Czech Republic, 2004.